



## Article

# Response of Long-Term Water and Phosphorus of Wheat to Soil Microorganisms

Junjie Hu, Yanhao Lian, Hui Guo, Zongzhen Li , Haifang Pang, Mengjiao Zhang, Yongzhe Ren, Tongbao Lin \*  and Zhiqiang Wang

College of Agriculture, Henan Agricultural University, Zhengzhou 450002, China; hjj17737146358@163.com (J.H.); wangcrops@sina.com (Z.W.)

\* Correspondence: linlab@163.com

**Abstract:** Phosphorus deficiency critically constrains crop growth. Soil microbial diversity, which is crucial for maintaining terrestrial ecosystem integrity, plays a key role in promoting soil P cycling. Therefore, it is imperative to understand the survival strategies of microorganisms under P-limited conditions and explore their roles in community regulation. We initiated a comprehensive, long-term, in situ wheat field experiment to measure soil physicochemical properties, focusing on the different forms of soil inorganic P. Subsequently, 16S rRNA and ITS marker sequencing was employed to study changes in soil microbial abundance and community structure and predict functional alterations. The results showed that soil water and P deficiencies significantly affected wheat growth and development, soil physicochemical properties, and microbial diversity and function. Prolonged P deficiency lowered soil pH, significantly increasing phosphatase content (58%) under W1 (normal irrigation) conditions. Divalent calcium phosphate decreased significantly under W0 (lack of irrigation) and W1 conditions, and the most stable ten-valent calcium phosphate began to transform under W0 conditions. Soil microbial diversity increased (e.g., *Proteobacteria* and *Vicinamibacterales*) and enhanced the transport capacity of bacteria. P deficiency affected the coexistence networks between bacteria and fungi, and SEM (structural equation modeling) analysis revealed a stronger correlation in bacteria ( $r^2 = 0.234$ ) than in fungi ( $r^2 = 0.172$ ). In soils deprived of P for 7 years, the soil P content and forms were coupled with microbial changes. Microorganisms exhibited community and functional changes in response to low-phosphorus soil, concurrently influencing soil P status. This study enhances our understanding of rhizospheric processes in soil P cycling under microbial feedback, particularly the impact of microbial interactions on changes in soil P forms under P-limited conditions.

**Keywords:** wheat; phosphorus deficiency; microbial diversity; microbial function; microbial interaction



**Citation:** Hu, J.; Lian, Y.; Guo, H.; Li, Z.; Pang, H.; Zhang, M.; Ren, Y.; Lin, T.; Wang, Z. Response of Long-Term Water and Phosphorus of Wheat to Soil Microorganisms. *Agriculture* **2024**, *14*, 2022. <https://doi.org/10.3390/agriculture14112022>

Academic Editor: Luciano Kayser Vargas

Received: 5 August 2024

Revised: 1 November 2024

Accepted: 2 November 2024

Published: 10 November 2024



**Copyright:** © 2024 by the authors. Licensee MDPI, Basel, Switzerland. This article is an open access article distributed under the terms and conditions of the Creative Commons Attribution (CC BY) license (<https://creativecommons.org/licenses/by/4.0/>).

## 1. Introduction

Water availability and P are critical determinants of the optimal growth of wheat [1,2], modulating both the physicochemical attributes of the soil and its biological processes, such as nutrient assimilation, molecular metabolism, and microbial activities [3,4]. Globally, wheat, a principal staple crop, addresses the fundamental energy requirements of over one-third of the world's population, boasting a cultivation area exceeding 220 million hectares [5–7]. Soil fertility in contemporary agricultural settings depends on extensive fertilizer applications. To increase agricultural productivity, phosphate resources are mined to produce phosphate fertilizers that significantly enhance crop growth. However, this approach presents challenges for environmental sustainability. Moreover, the rapid decline in phosphate deposits has raised concerns about the sustainability of phosphate fertilizer production from phosphate ores. As reserves decrease, the cost of mining and processing may continue to rise, affecting the future affordability and stability of phosphate supplies [8]. P is an indispensable element for wheat development and function. As one of the 17 mineral elements essential for crop productivity, P is intricately involved in nutrient

provision and multiple metabolic pathways [9]. However, the excessive deployment of phosphatic fertilizers causes a widespread P surplus in the global agricultural terrain, subsequently compromising fertilizer utilization efficiency and agronomic P equilibrium [10]. Additionally, considering the primary derivation of phosphatic fertilizers from phosphate rock, a finite resource, it is noteworthy that the bulk of P introduced into agricultural soils remains biologically unassimilated post-application. Sequestration reactions limit P mobility, categorizing it among the most immobile, least accessible, non-bioavailable, and non-renewable nutrients [11,12]. Experts have anticipated the depletion of global phosphate rock reserves by the end of this century. Specific studies indicate that, in the calcareous soils of Northern China, inorganic soil P typically constitutes 50–80% of the TP (total P), with Ca-P dominating the inorganic fraction, accounting for over 80%, primarily as Ca<sub>10</sub>-P. Water is an elemental lifeline for wheat [13]. Meanwhile, moisture plays a crucial role in phosphorus acquisition. Suitable moisture can improve the solubility and bioavailability of phosphorus. Historically, research efforts have predominantly focused on the ecological ramifications of these factors, exploring optimal water–fertilizer management strategies and seasonal impacts, with relatively few studies on soil productivity [14]. Soil ecosystems with diverse microbial communities profoundly influence soil functions. However, in the context of expansive wheat cultivation, microbial responses to water and P dynamics and their subsequent implications for the exploration of soil P reservoirs remain under-investigated.

The combination of fungi and bacteria is an important component of the soil microbiome. Fungi secrete enzymes to initiate the decomposition of organic matter and establish a synergistic relationship with bacteria, such as arbuscular mycorrhizal fungi and bacteria. Fungi provide bacteria with a carbon source that supports their growth, whereas bacteria promote the uptake of P and other nutrients by fungi. Together, these interactions regulate soil nutrient cycling and ecosystem functions that, in turn, affect plant-related chemical processes and soil ecosystem services [15]. P fertilizers have the potential to alter soil microbial attributes, including the quantity, diversity, abundance, and composition of bacteria and fungi [16]. A study on grassland soils revealed that long-term P fertilizer application can enhance bacterial community diversity and the expression of prokaryotic alkaline phosphatase (*phoD*) genes [17]. Another investigation identified that P fertilization notably elevated the diversity and abundance of most genes associated with P cycling and influenced species evenness and key genera within the community [18]. P fertilization significantly affects the structure of soil microbial communities and certain rare microbial taxa [19]. A comprehensive understanding of the community dynamics of soil bacteria and fungi along with their interactions with the surrounding environment is of paramount importance for the efficiency of water and P utilization. Contemporary research endeavors have predominantly emphasized harnessing rhizospheric microbial communities to bolster the sustainability of food production. Emerging evidence suggests that plant-associated microbiomes ameliorate plant responses to drought-induced stress. Plants have evolved an array of adaptive strategies, collectively termed as the P starvation response, to optimize P utilization and enhance P acquisition under P-deficient conditions. These strategies involve various growth, development, and metabolic processes. Intriguingly, plant responses evolved in the context of P starvation response have intricate associations with microbial activity [20]. For instance, maize (*Zea mays* L.) and *Arabidopsis thaliana* have adopted the strategy of increasing lateral root number under P deficiency [21]. Therefore, gaining insights into the responses and adaptations of soil microbes to conditions of drought and P deficiency has profound ecological significance.

We conducted a longitudinal study on winter wheat using fixed water and fertilizer treatments. Utilizing 16S rRNA and ITS marker sequencing, we delineated bacterial and fungal community structures, respectively. Although there is a foundational understanding of plant–microbe rhizospheric interactions and the impact of microbes on plant growth and development, research under specific water and P conditions remains limited. Our primary objectives were to (1) discern the influence of water and P regimes on wheat

growth development and soil P fractions, (2) elucidate the effects of water and P dynamics on microbial community structures, and (3) prognosticate the functional implications of soil microbes under varying water and P conditions. The overarching aim was to enhance the understanding of the intricate interplay between the soil environment and microbial composition and functionality, thereby refining management practices for sustainable agricultural ecosystems and soil health.

## 2. Materials and Methods

### 2.1. Site Description and Experimental Design

The study site was located at the Yuanyang Ecology Experimental Station of Henan Agricultural University (113°85' N, 35°31' E) in Henan province, China, which has a warm, temperate, semi-humid continental monsoon climate and good land cultivation conditions. The daily average temperature is approximately 14.5 °C, annual average sunshine duration is 1925.1 h, and annual average temperature is above 10 °C for approximately 230 days.

The experimental cropping system was a wheat–maize rotation, high yield and high-quality dwarf resistance, with extensive planting in Huang-Huai area AK58. In October 2015, treatments were initiated to investigate the effects of irrigation and P application. Finally, we collected soil samples solely from the last wheat season (2021–2022) to measure the indicators. The study design included two irrigation methods, no irrigation (W0) and irrigation during wintering and jointing (W1), and two P dosages (0 and 120 kg ha<sup>-1</sup> designated P0 and P1, respectively). A total of 4 treatments (W0P0, W0P1, W1P0, W1P1) were applied. The experiments were performed in an area of 35.6 × 42.6 m divided into plots of 7.1 m × 16.8 m, with three replicates per treatment. The N, P, and K forms applied were urea (240 kg ha<sup>-1</sup>), calcium superphosphate (120 kg ha<sup>-1</sup>), and potassium chloride (120 kg ha<sup>-1</sup>). All fertilizers were spread manually before sowing.

### 2.2. Soil Sample Collection

Soil samples for microbiological and soil analyses were obtained as follows: (1) Inter-row soil: First, the litter on the ground was removed, and a 0–15 cm deep core was extracted midway between rows with a soil auger and subsequently sieved through a 2 mm mesh. For each farmland, soil samples from 10 randomly selected locations were combined to form a composite sample representative of each farmland; soil fertility index was determined by inter-row soil with six replicates per treatment. (2) Rhizospheric soil: In each farmland, 10 plants were selected randomly from those adjacent to where the inter-row soil was collected. These plants were completely removed, and mud chunks from their roots were removed. This left only the soil attached to the roots, which, in turn, was gently shaken off, collected, sieved through a 2 mm mesh, and mixed into a composite sample per farmland. From these composite samples of inter-row soil and rhizospheric soil, a portion of each was quickly transferred into a 15 mL sterile centrifuge tube, sealed immediately, and transported on dry ice to the laboratory where these samples were stored at –80 °C in an ultra-low-temperature refrigerator until microbiological analysis. Simultaneously, inter-row soil samples were retained as fresh samples for the determination of nitrate and ammonium nitrogen, and the remaining soil was dried to determine its physical and chemical properties.

### 2.3. Soil Environment Factor

The soil pH was measured using a pH meter. The organic matter (SOC) content was determined using the dichromate oxidation method. TN (total soil nitrogen) was quantified using the modified Kjeldahl method. The concentrations of NH<sub>4</sub><sup>+</sup> and NO<sub>3</sub><sup>-</sup> in the soil, extracted with 2 M KCl (Sinopharm Chemical Reagent Co., Ltd., Shanghai, China, all consumables for this test were obtained from this supplier), were determined using a continuous flow system (Santt System, Skalar, Breda, The Netherlands). AvK (available soil potassium) was measured using flame photometry. Both TP (total phosphorus) and AvP (available phosphorus) in the soil were determined using the molybdenum blue colorimetric

method [22]. Olsen-P was determined by extracting air-dried soil with  $0.5 \text{ mol L}^{-1} \text{ NaHCO}_3$  at pH 8.5. Soil Pi fractionation was performed according to a fractionation scheme for calcareous soils based on previously described methods [23,24]. In the Pi fractionation scheme, soil Pi was divided into six fractions as  $\text{Ca}_2\text{-P}$ ,  $\text{Ca}_8\text{-P}$ ,  $\text{Al-P}$ ,  $\text{Fe-P}$ , occluded P, and  $\text{Ca}_{10}\text{-P}$  using a sequential extraction procedure with (1)  $0.25 \text{ mol L}^{-1} \text{ NaHCO}_3$  solution at pH 7.5 to remove  $\text{Ca}_2\text{-P}$ , (2)  $0.5 \text{ mol L}^{-1} \text{ NH}_4\text{Ac}$  at pH 4.2 to remove  $\text{Ca}_8\text{-P}$ , (3)  $0.5 \text{ mol L}^{-1} \text{ NH}_4\text{F}$  at pH 8.2 to remove  $\text{Al-P}$ , (4)  $0.1 \text{ mol L}^{-1} \text{ NaOH}$ - $0.1 \text{ mol L}^{-1} \text{ Na}_2\text{CO}_3$  to remove  $\text{Fe-P}$ , (5)  $0.3 \text{ mol L}^{-1} \text{ Na}_3(\text{citrate})\text{-Na}_2\text{S}_2\text{O}_4$ - $0.5 \text{ mol L}^{-1} \text{ NaOH}$  solution to remove occluded P, and (6)  $0.25 \text{ mol L}^{-1} \text{ H}_2\text{SO}_4$  to remove  $\text{Ca}_{10}\text{-P}$ .

#### 2.4. Measurements of Photosynthesis-Related Parameters

Gas exchange parameters of photosynthesis that included net photosynthetic rate ( $P_n$ ), stomatal conductance ( $G_s$ ), and transpiration rate ( $Tr$ ) were measured with a portable Li-6400 photosynthesis system (LI-COR, Shanghai Ditu Biotechnology Co., Ltd., Shanghai, China) at a flow rate of  $400 \mu\text{mol s}^{-1}$ , an atmospheric  $\text{CO}_2$  concentration, and  $1200 \text{ mmol m}^{-2} \text{ s}^{-1}$  photosynthetically active radiation in a  $2 \times 3 \text{ cm}^2$  area. The measurements were recorded after equilibration to a steady state in which  $G_s$  and  $Tr$  were positive and  $P_n$  was stable at one decimal place and no longer increased or decreased. The experimental measurements were taken at 0, 7, 14, 21, 28, and 35 days after the flowering period, and the index measurements were taken between 9 a.m. and 11 a.m., when the sky was not cloudy. Leaves with the same growth and light direction were selected in the field, 20 flag leaves were measured in each sample plot, and the highest photosynthesis value in the different treatments was selected. Photosynthetic N-use efficiency (PNUE) was calculated as follows:

$$\text{PNUE} = P_n / \text{LN}.$$

#### 2.5. DNA Extraction, PCR Amplification, and Sequencing

Wheat rhizosphere soil samples were collected using the different treatments. Microbial DNA was extracted from 0.5 g soil samples (fresh weight) using an E.Z.N.A. soil DNA Kit (Omega Bio-Tek, Norcross, GA, USA). The final DNA concentration was determined using a NanoDrop 2000 UV-vis spectrophotometer (Thermo Fisher Scientific, Wilmington, DE, USA), and DNA quality was confirmed by 1% agarose gel electrophoresis. Bacterial DNA was amplified using the 16S rRNA (V3 + V4) region primers: (338F: 5'-ACTCCTACGGGAGGCAGCA-3', and 806R:5'-GGACTACHVGGGTWTCTAAT-3') [24]. Fungal DNA was amplified using the ITS region (internal transcribed spacer) primers: (ITS1F: 5'-CTTGGTCATTTAGAGGAAGTAA-3', and ITS2R: 5'-GCTGCGTTCTTCATCGATGC-3') [25]. Finally, the DNA was sent to the company for high-throughput sequencing.

#### 2.6. Processing of Sequencing Data

Data preprocessing involved the following three steps:

**Quality filtering:** Initially, Trimmomatic v0.33 software (Beijing Baimai Cloud Technology Co., Ltd., Beijing, China) was used to filter the raw reads obtained from sequencing with the following criteria: (1) The quality scores of the reads were screened using a quality threshold of Q20; (2) Reads containing ambiguous bases were removed, and primers were matched exactly allowing two nucleotides. Cutadapt 1.9.1 software was then used to identify and remove primer sequences, resulting in clean reads without primer sequences.

**Paired-end sequence merging:** USEARCH v10 software was used to merge the clean reads of each sample based on overlap. The merged data were then subjected to length filtering according to the length range of different regions.

**Chimeric removal:** UCHIME v4.2 software was used to identify and remove chimeric sequences, resulting in a final set of effective reads. USEARCH software was utilized to cluster the reads at a 97.0% similarity threshold, generating operational taxonomic units (OTUs). Taxonomic annotation of the OTUs was performed using the naive Bayes classifier (threshold is set to 0.7), with SILVA 138 as the reference database. This annotation provided



species classification information for each feature, enabling the compilation of community compositions at various taxonomic levels (phylum, class, order, family, genus, and species) using QIIME 2 software.

### 2.7. Statistical Analyses

Soil data and microbial community data at the phylum and genus levels were organized using Microsoft Excel 2020. IBM SPSS Statistics 25 was used for variance comparison, and the LSD test was employed for significance testing ( $p < 0.05$ ). The species abundance histogram and NMDS analysis under different treatments were performed using BMK-Cloud ([www.biocloud.net](http://www.biocloud.net), accessed on 1 November 2024). Spearman's correlation analysis was conducted, and heatmap visualization was performed using GraphPad Prism 8. Visualization of co-occurrence networks was performed using R 4.1.3. To assess the overall effect of environmental factors on microbial community structure, we correlated the distance matrix of environmental variables and microbial community structure using Mantel analysis. To determine the significance of the relationship between specific environmental variables and microbial diversity, a Wald-type  $\chi^2$  test was applied to analyze individual variables within the linear mixed-effects model. Bacterial and fungal functional predictions were carried out using R 4.1.3 with Tax4Fun2 [26]. The co-occurrence network analysis results were also visualized using R 4.1.3 with the 'psych' package, followed by Gephi to beautify the images. Image editing and processing were performed using Adobe Photoshop 2021. SEM was performed using SmartPLS 4.0.

## 3. Results

### 3.1. Wheat Yield and Photosynthesis

The W1P0, W0P1, and W1P1 treatments showed significant yield increases of 17.6%, 23.12%, and 66.09%, respectively, compared to the W0P0 treatment. The W1P0, W0P1, and W1P1 treatments increased the spike number by 52.16%, 26.75%, and 88.14%, respectively, and the 1000-grain weight increased by 20.34%, 9.81%, and 19.88%; the kernel number increased by 7.14%,  $-5.4\%$ , and 2.47% (Table 1). Compared with P1, the Pn, Tr, and Gs (the average value of the two W treatments) of the P0 treatment decreased by 20.03%, 36.78%, and 16.80%, respectively, which were significant differences. Although the water and phosphorus treatments showed no significant interaction, each had a significant effect on most of the indicators.

**Table 1.** Effects of water and phosphorus on yield and photosynthetic characteristics of wheat.

Treatment	Spike Number ( $10^4 \text{ ha}^{-1}$ )	1000-Kernel Weight (g)	Kernel Number (per Ear)	Yield ( $\text{kg ha}^{-1}$ )	Photosynthetic Rate ( $\mu\text{mol m}^{-2}\cdot\text{s}^{-1}$ )	Transpiration Rate ( $\text{mmol m}^{-2}\cdot\text{s}^{-1}$ )	Stomatal Conductance ( $\text{mmol m}^{-2}\cdot\text{s}^{-1}$ )
W0P0	339.3 $\pm$ 5.25 c	39.23 $\pm$ 0.34 b	39.20 $\pm$ 2.27 ab	4437.15 $\pm$ 18.97 c	10.03 $\pm$ 1.74 b	2.18 $\pm$ 0.54 b	0.14 $\pm$ 0.04 b
W1P0	399.3 $\pm$ 23.35 ab	47.21 $\pm$ 3.54 a	42.00 $\pm$ 4.60 a	6751.8 $\pm$ 62.49 ab	14.68 $\pm$ 1.21 a	4.01 $\pm$ 0.27 a	0.34 $\pm$ 0.06 a
W0P1	417.75 $\pm$ 60.3 b	43.08 $\pm$ 0.68 ab	37.07 $\pm$ 2.19 b	5624.1 $\pm$ 85.06 bc	6.53 $\pm$ 2.17 c	1.15 $\pm$ 0.35 c	0.07 $\pm$ 0.02 c
W1P1	568.55 $\pm$ 56.36 a	47.03 $\pm$ 0.92 a	40.17 $\pm$ 3.20 a	8348.25 $\pm$ 90.53 a	12.95 $\pm$ 1.52 a	3.59 $\pm$ 0.41 a	0.3 $\pm$ 0.04 a
W	*	**	ns	**	**	**	**
P	*	ns	ns	**	**	*	**
W $\times$ P	ns	ns	ns	ns	ns	ns	ns

Values are means  $\pm$  se ( $n = 6$ ). Values followed by different letters within each column are significantly different at the probability level of 0.05. ns, not significant, \*  $p < 0.05$ , \*\*  $p < 0.01$ .

### 3.2. Changes in Soil Properties

The effects of water and P deficiencies on soil chemistry were also observed (Table 2). Under both W0 and W1 conditions, P1 significantly increased the soil pH compared with P0. Under W0 conditions, long-term P deficiency resulted in a 14% reduction in TP content as well as significant decreases in  $\text{NO}_3^- \text{N}$ ,  $\text{NH}_4^+ \text{N}$ , AvK, and AvP content. However, under W1 conditions, the impact on TP was not statistically significant. Lack of water and P also influenced the different forms of P present in the soil (Table 2). Under W0 conditions, phosphorus deficiency resulted in a 6% reduction in Al-P, 14.09% reduction in Fe-P, and 3.47% reduction in O-P.  $\text{Ca}_2\text{-P}$ ,  $\text{Ca}_8\text{-P}$ , and  $\text{Ca}_{10}\text{-P}$  levels showed significant changes. Under

W1 conditions, P0 compared with P1 caused a 3.55% reduction in Al-P and Fe-P, while Ca<sub>2</sub>-P reached a significant level. O-P, Ca<sub>8</sub>-P, and Ca<sub>10</sub>-P remained relatively stable; in particular, Ca<sub>2</sub>P and Ca<sub>10</sub>P played a significant role in water–P interactions, suggesting that water availability can mitigate the effects of low P in the soil.

**Table 2.** Effects of water and phosphorus on soil physicochemical properties.

Treatment	W0P0	W0P1	W1P0	W1P1	p Value		
					W	P	W × P
pH	7.64 ± 0.09 b	7.89 ± 0.23 a	7.63 ± 0.15 b	7.9 ± 0.23 a	<0.001	<0.001	0.043
TC (g kg <sup>-1</sup> )	7.99 ± 0.1 a	7.46 ± 0.23 a	7.61 ± 0.41 b	7.02 ± 0.45 a	0.06	0.871	0.018
TN (g kg <sup>-1</sup> )	1.04 ± 0.05 a	0.95 ± 0.06 a	0.97 ± 0.02 a	0.87 ± 0.01 a	0.013	0.999	0.004
TP (g kg <sup>-1</sup> )	0.85 ± 0.07 a	1.18 ± 0.06 a	0.83 ± 0.08 a	1.18 ± 0.05 a	0.046	<0.001	<0.001
NO <sub>3</sub> <sup>-</sup> N (mg kg <sup>-1</sup> )	5.3 ± 0.33 b	5.91 ± 0.57 a	4.96 ± 0.57 b	6.36 ± 0.67 b	0.863	0.252	0.013
NH <sub>4</sub> <sup>+</sup> N (mg kg <sup>-1</sup> )	12.29 ± 0.38 b	16.21 ± 0.6 a	15.44 ± 1.41 a	17.26 ± 2.01 a	0.022	0.193	0.05
AvP (mg kg <sup>-1</sup> )	1.98 ± 0.25 b	6.89 ± 0.55 a	4.25 ± 0.07 b	9.43 ± 0.84 a	<0.001	0.651	<0.001
AvK (mg kg <sup>-1</sup> )	72.63 ± 11.36 b	103.03 ± 4.3 a	63.88 ± 22.72 b	88.59 ± 25.82 a	0.303	0.794	0.031
PA (ug(g.24 h) <sup>-1</sup> )	918.82 ± 90.35 b	1042.55 ± 105.95 a	956.13 ± 315.35 b	1514.44 ± 301 a	0.09	0.139	0.033
UA (ug(g.2 h) <sup>-1</sup> )	52.65 ± 14 a	57.81 ± 2.83 a	46.91 ± 1.99 a	47.89 ± 5.46 a	0.117	0.651	0.51
SA (mg(g.24 h) <sup>-1</sup> )	60.36 ± 9.71 a	58.73 ± 12.61 a	54.54 ± 5.6 a	49.25 ± 3.88 a	0.164	0.723	0.508
Al-P (mg kg <sup>-1</sup> )	44.24 ± 1.76 a	47.35 ± 1.07 a	41.33 ± 2.11 a	42.85 ± 3.36 a	0.021	0.11	0.055
Fe-P (mg kg <sup>-1</sup> )	33.78 ± 1.67 b	39.32 ± 1.67 ab	35.92 ± 2.08 b	42.25 ± 4.35 a	0.141	0.005	0.805
O-P (mg kg <sup>-1</sup> )	62.28 ± 1.88 a	64.52 ± 2.61 a	64.05 ± 2.32 a	64.61 ± 1.59 a	0.473	0.29	0.516
Ca <sub>2</sub> -P (mg kg <sup>-1</sup> )	4.96 ± 1.02 cd	20.35 ± 2.44 a	5.2 ± 0.08 cd	11.64 ± 3.42 b	0.009	<0.001	0.007
Ca <sub>8</sub> -P (mg kg <sup>-1</sup> )	114.78 ± 10.61 bc	130.52 ± 17.14 a	119.05 ± 4.97 b	108.06 ± 4.53 bc	0.177	0.709	0.061
Ca <sub>10</sub> -P (mg kg <sup>-1</sup> )	54.74 ± 3.15 b	202.16 ± 9.95 a	207.67 ± 16.18 a	201.37 ± 0.93 a	<0.001	<0.001	<0.001

Values are means ± se (*n* = 3). Different lowercase letters after the same column of data indicate significant difference between different treatments for the same factor (*p* < 0.05). TC is soil organic carbon, TN is total nitrogen, TP is total phosphorus, AvP is available phosphorus, AvK is average potassium, PA is phosphatase activity, UA is urease activity, and SA is sucrase activity.

### 3.3. Bacterial and Fungal Diversity Index and Abundance

After quality control, 927,058 effective tags were obtained for bacterial 16S rRNA gene sequencing, whereas fungal ITS gene sequencing yielded 944,318 effective tags. The influence of water and P on the soil bacterial and fungal communities was evident (Figure S1). Rarefaction curve analysis indicated that the bacterial 16S curve plateaued at 927,058 sequences (Figure S2a), whereas the fungal ITS gene curve reached saturation at 944,318 sequences (Figure S2b).

Alpha diversity indices were calculated at the OTU level to quantify the microbial community diversity and richness (Table 3). For both bacteria and fungi, all water treatments exhibited increased OTUs and ACE, Chao 1, and Shannon indices compared with the control group. For bacteria, under normal water conditions, the P1 treatment demonstrated higher OTUs and ACE and Chao 1 indices than the P0 treatment, with the exception of the Shannon index. Under the W0 condition, the P0 treatment exhibited higher OTUs than the P1 treatment, whereas the remaining indices were higher in the P1 treatment than in the P0 treatment. For fungi, under the W1 condition, the low-P treatment had higher OTUs and Shannon index, whereas the ACE and Chao 1 indices showed opposite results. Under W0 conditions, the P1 treatment exhibited higher values for all indexes than the P0 treatment.

The similarity of bacterial and fungal communities among the samples was assessed using Anosim and NMDS techniques based on the Bray–Curtis distance metric. The addition of water and P resulted in significant shifts in the community structure of soil bacteria and fungi, leading to distinct differences between the treatments (Figure S1a; Anosim, *r* = 0.54, *p* = 0.001; Figure S1b, *r* = 0.79, *p* = 0.001). In conclusion, P and water influenced the diversity and richness of soil microorganisms.

**Table 3.** Effects of water and phosphorus on soil microbial alpha-diversity.

Microorganism	Treatment	OTU Richness	ACE Index	Chao1 Index	Shannon Index
Bacteria	W0P0	1942.3 ± 30.7 ab	1948.56 ± 12.53 c	1966.05 ± 10.27 c	9.37 ± 0.01 c
	W0P1	1919.7 ± 4.0 b	1956.41 ± 3.73 c	1971.04 ± 6.44 bc	9.39 ± 0.03 c
	W1P0	1943.3 ± 9.9 ab	1975.46 ± 9.18 a	1989.23 ± 13.79 b	9.63 ± 0 a
	W1P1	1967.7 ± 7.0 a	1997.17 ± 6.76 b	2012.2 ± 8.10 a	9.51 ± 0.01 b
Fungus	W0P0	274 ± 19.92 b	290.42 ± 22.87 c	305.44 ± 26 c	3.72 ± 0.24 c
	W0P1	282.3 ± 13.20 b	318.7 ± 23.91 bc	326.61 ± 28.76 bc	4.35 ± 0.07 b
	W1P0	337.7 ± 7.02 a	355.26 ± 8.16 ab	360.64 ± 9.63 ab	5.07 ± 0.27 a
	W1P1	334.7 ± 9.29 a	366.26 ± 22.11 a	384.04 ± 37.72 a	4.51 ± 0.39 b

Values are mean ± SD ( $n = 3$ ). Different letters in the same column indicate a significant difference at  $p < 0.05$ .

### 3.4. Composition of the Bacterial and Fungal Communities

The dominant bacterial phyla observed in the W1P1 treatment across all soil samples were *Proteobacteria* (36.04%), *Acidobacteriota* (23.45%), *Actinobacteriota* (12.25%), *Bacteroidota* (7.59%), and *unclassified\_Bacteria* (4.78%), which collectively accounted for over 80% of all sequences. Other prominent phyla included *Gemmatimonadota* (4.92%), *Myxococcota* (2.57%), *Methylomirabilota* (1.81%), *Chloroflexi* (2.13%), and *Verrucomicrobiota* (0.99%) (Figure 1a). Regardless of the W1 or W0 conditions, P deficiency led to an increased relative abundance of *Acidobacteriota*, *unclassified\_Bacteria*, *Myxococcota*, *Methylomirabilota*, and *Chloroflexi* among the top ten phyla. Conversely, P deficiency resulted in a decreased relative abundance of *Proteobacteria*, *Actinobacteriota*, and *Bacteroidota*. In the W1P1 treatment, the dominant bacterial genera were *Vicinamibacterales* (7.30%), *Vicinamibacteraceae* (6.93%), *unclassified\_Bacteria* (4.78%), *Sphingomonas* (4.94%), *Gemmatimonadaceae* (3.45%), *Massilia* (3.75%), *RB41* (1.70%), *MND1* (17.3%), *Lysobacter* (2.32%), and *gamma\_proteobacterium* (1.16%), accounting for less than 40% of all sequences (Figure 1b). Under W1 conditions, P deficiency increased the abundance of *Vicinamibacterales*, *Vicinamibacteraceae*, *unclassified\_Bacteria*, *Gemmatimonadaceae*, *RB41*, and *MND1* and decreased the abundance of *Sphingomonas*, *Massilia*, and *Lysobacter*. Under W0, P deficiency increased the abundance of *Vicinamibacterales*, *unclassified\_Bacteria*, *Gemmatimonadaceae*, *Massilia*, *RB41*, *MND1*, and *gamma\_proteobacterium* while simultaneously decreasing the abundance of *Vicinamibacteraceae*, *Sphingomonas*, and *Lysobacter*. In addition to the differences at the phylum level, the treatments altered the abundance of bacterial taxa (Figure S3a,c).

In the W1P1 treatment, the dominant fungal phyla among the top ten taxa were *Ascomycota* (43.37%), *Basidiomycota* (50.57%), *Mortierellomycota* (3.05%), *unclassified\_Fungi* (1.02%), *Glomeromycota* (0.17%), and *Chytridiomycota* (0.49%), accounting for 99% of all sequences (Figure 1c). Under normal water conditions, P deficiency increased the abundance of *Ascomycota*, *unclassified\_Fungi*, and *Glomeromycota* and decreased the abundance of *Basidiomycota* and *Mortierellomycota* at the phylum level. Under water-deficient conditions, P deficiency increased the abundance of *Glomeromycota* and *Chytridiomycota*, whereas it decreased the abundance of *Mortierellomycota* and *unclassified\_Fungi*. Among the fungal community at the genus level, the top ten dominant genera were *Filobasidium* (31.73%), *Scytalidium* (6.9%), *Cladosporium* (15.15%), *Fusarium* (4.76%), *Alternaria* (8.96%), *Vishniacozyma* (8.09%), *Acremonium* (0.31%), *Cystofilobasidium* (3.80%), *Mortierella* (3.05%), and *Coprinopsis* (1.31%). These genera collectively accounted for a total abundance of 77% (Figure 1d). Under normal water conditions, P deficiency increased the abundance of *Scytalidium*, *Acremonium*, and *Coprinopsis*. Under drought conditions, P deficiency increased the abundance of *Filobasidium*, *Scytalidium*, and *Acremonium*. In addition to the differences at the phylum and genus levels, a subset of fungi was enriched in all four treatments (Figure S3b,d).

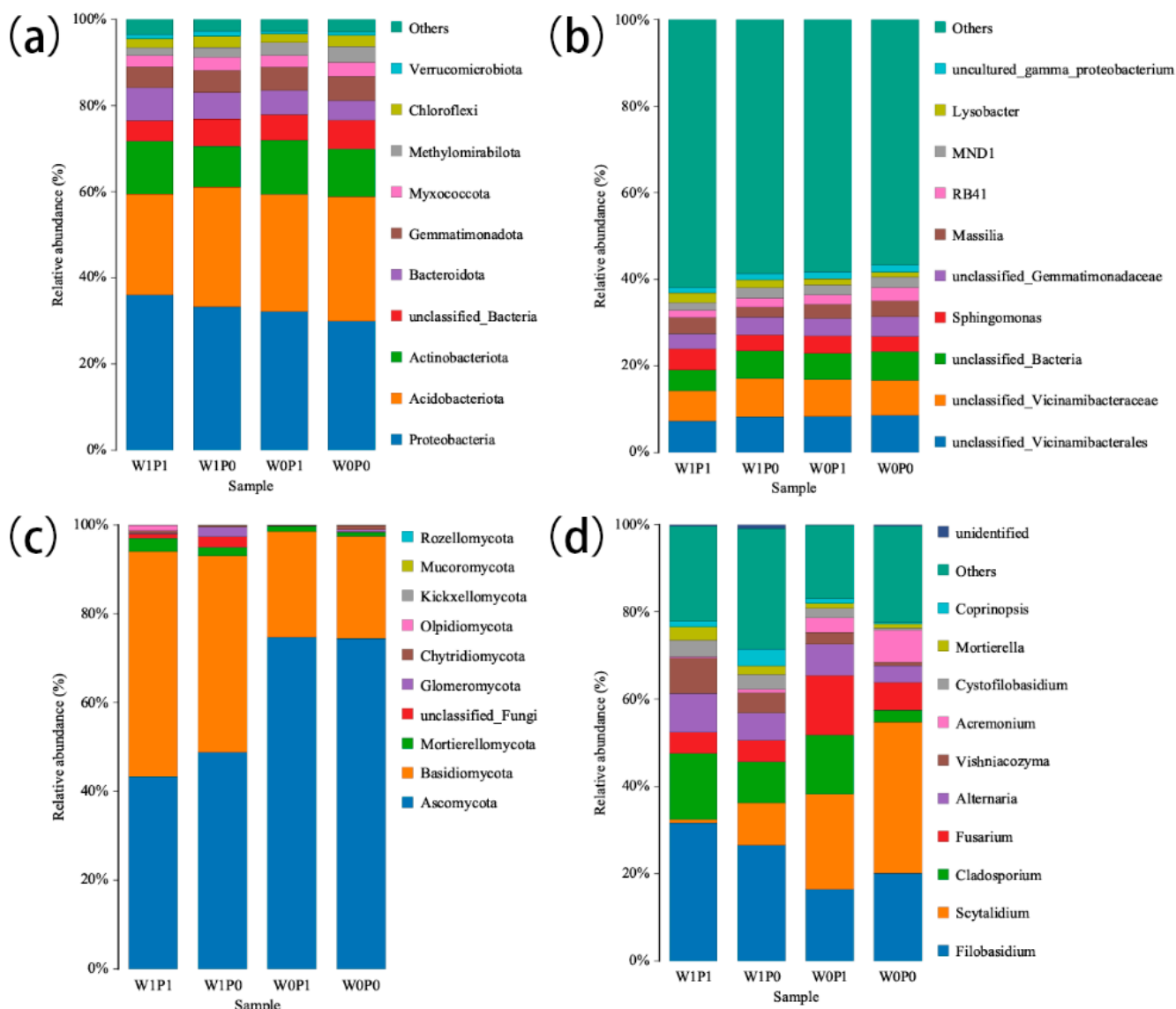


**Figure 1.** Relative abundances of dominant bacterial phyla (a), bacterial genera (b), fungal phyla (c), and fungal genera (d).

### 3.5. Prediction of Fungal and Bacterial Function

Significant variations in the secondary functions of bacteria and fungi were evident across the different treatments, as indicated by the abundance of soil bacteria and their functions based on KEGG data (Figure 2). Under drought conditions, notable distinctions were observed in the secondary functions of bacteria, including cellular processes, genetic information processing, metabolism, and organismal systems, among the various P treatments. Moreover, under normal water conditions, additional disparities were observed in environmental information processing compared with drought conditions. Conversely, the differences in the secondary functions of fungi were relatively fewer than those of bacteria, with significant differences in the predicted secondary functions observed primarily in cellular processes and metabolism but only under drought conditions.

Considering the classification of bacterial tertiary functions, significant differences were observed among soil bacteria under different P treatments during drought conditions. Specifically, compared with P1, several metabolic functions, such as transcription, chemical structure transformation maps, metabolism of terpenoids and polyketides, and development, exhibited significant increases in P0. The enhanced relative abundance of

these metabolic functions in soil bacteria plays a critical role in maintaining soil stability under drought and severe P deficiency conditions. Under normal water conditions, a greater variation in metabolic functions was observed among the different P treatments. Significant increases in cell growth and death, transport and catabolism, chemical structure transformation maps, metabolism of other amino acids, and xenobiotic biodegradation and metabolism were observed under the P0 condition. In fungi, several metabolic functions, such as transcription, replication and repair, carbohydrate metabolism, amino acid metabolism, and excretory system exhibited positive effects and significant increases under P-deficient conditions. However, under normal water conditions, although differences in the multiple metabolic functions of the fungi were observed, they did not reach statistical significance. This suggests that water availability exerts a more pronounced influence on fungi than P.

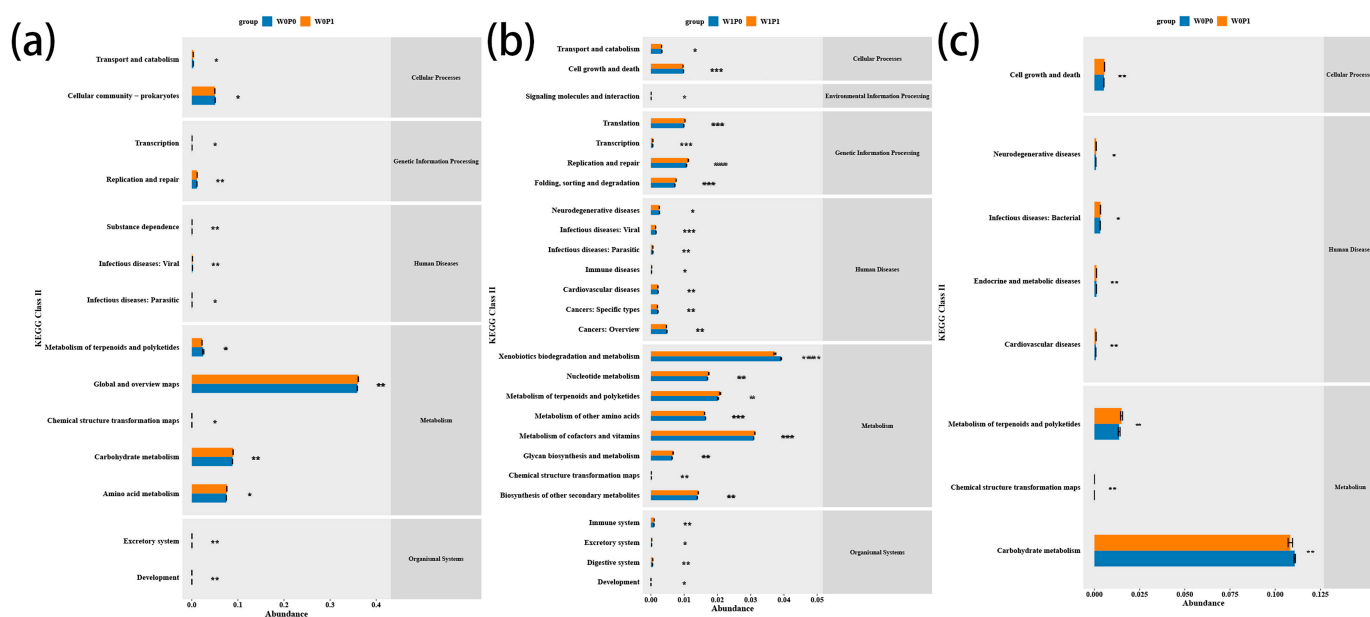


**Figure 2.** Differences in KEGG function of wheat soil bacteria (a,b) and fungi (c) (secondary and tertiary). For the above results, we retained only those that were significantly different between groups. Values are means  $\pm$  se ( $n = 3$ ). \*, \*\*, and \*\*\* indicate a difference at the 0.05, 0.01, and 0.001 levels, respectively.

### 3.6. Link Between Microbial Biodiversity and Soil Environmental Factors

We hypothesize that alterations in soil environmental conditions would exert a significant influence on microbial diversity under low-P drought conditions. Notably, our findings demonstrate a robust association between fungal abundance and levels of nitrate, nitrogen, and phosphatase content ( $r \geq 0.4$ ,  $p < 0.001$ ), whereas bacterial abundance displayed a noteworthy correlation with the concentrations of inorganic P species (aluminum phosphate and divalent calcium phosphate), phosphatase activity, and urease activity ( $r = 0.2\text{--}0.4$ ,  $p < 0.005$ ) (Figure 3).

Spearman’s correlation analysis was performed to evaluate the relationships between environmental factors and selected bacterial and fungal taxa (Figure 4). Most dominant bacteria and fungi were associated with at least one environmental factor. Among the bacteria, *Proteobacteria* showed a significant positive correlation with TP, AvN, AvP, and Pa and showed a positive correlation with the yield; however, this was not significant. Among the fungi, *Olpidiomycola* showed a significant positive correlation with pH, TP, AvN, AvP, Ca<sub>2</sub>P, Pa, and the yield.



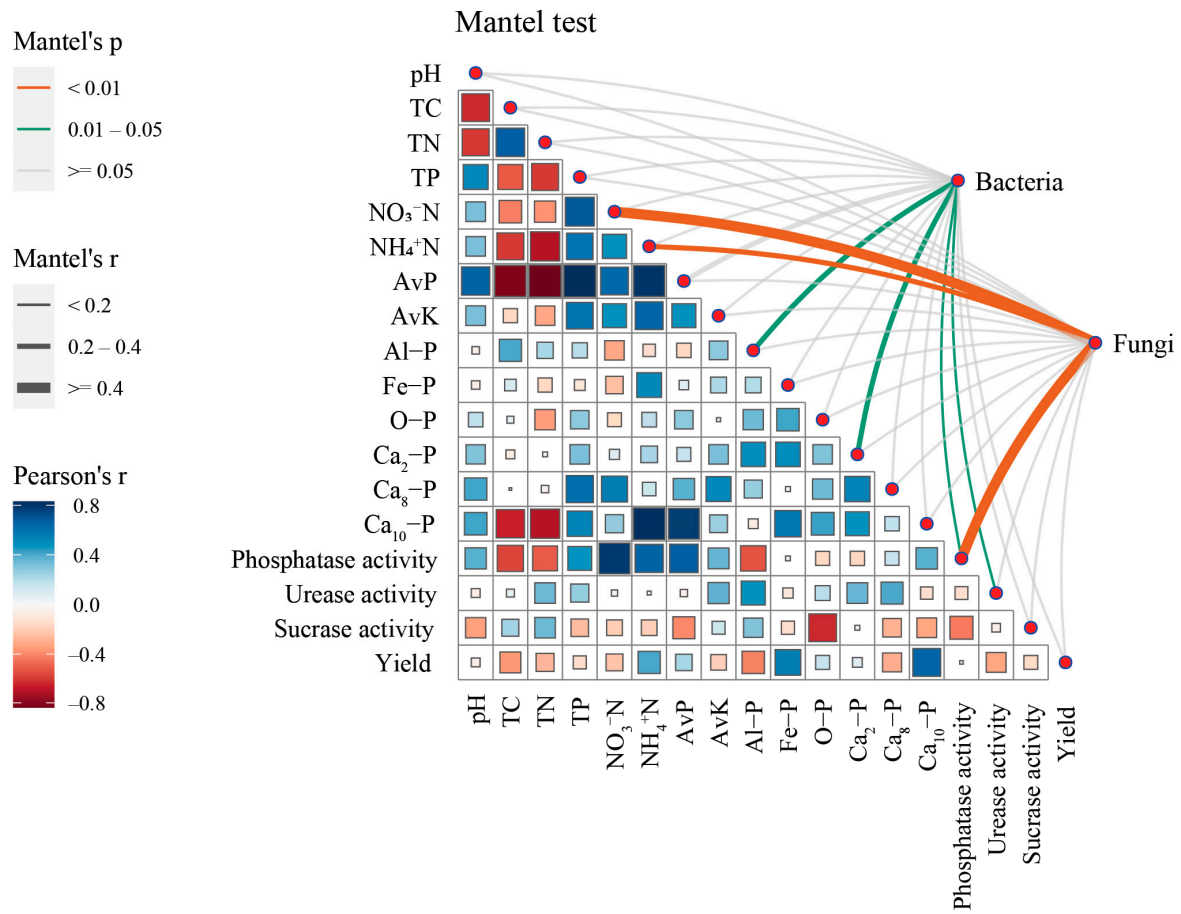


**Figure 3.** Environmental drivers of microbial diversity. Correlations between environmental variables and microbial diversity. Edge width corresponds to the absolute value of the correlation coefficient determined by the linear mixed-effects models. Colors indicate correlation types. Solid and dashed lines denote significant and non-significant correlations, respectively, based on Wald type II  $\chi^2$  tests. Pairwise comparisons of environmental factors are shown in the triangle, with a color gradient denoting Pearson's correlation coefficient.

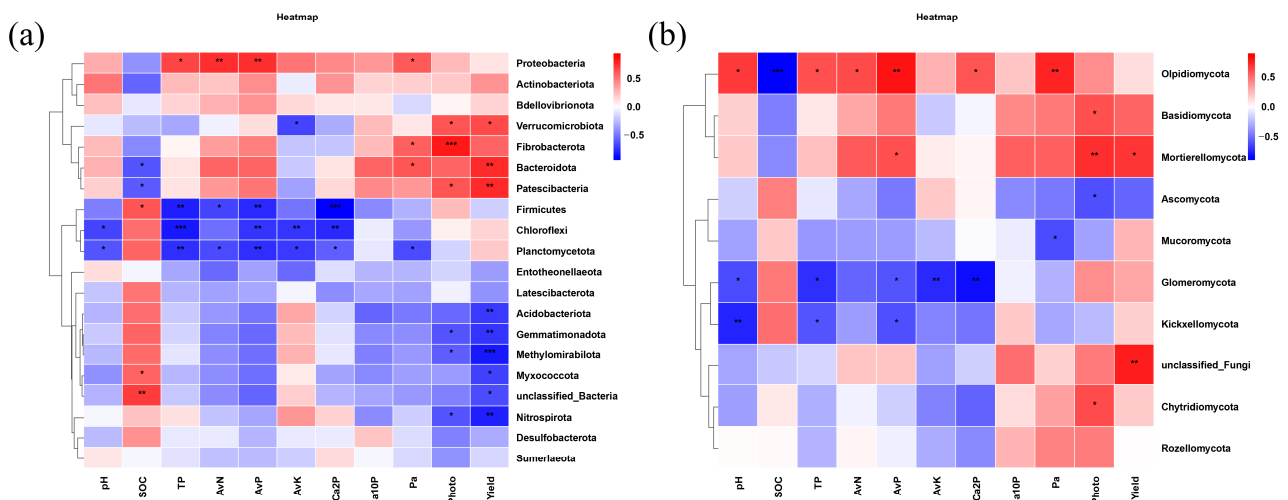


**Figure 4.** Spearman correlation heatmap between bacterial (a) and fungal (b) communities and soil properties and wheat photosynthetic characteristics. R-values are displayed in different colors, as indicated by the color code on the right of the heatmap. \*, \*\*, and \*\*\* indicate a difference at the 0.05, 0.01, and 0.001 levels, respectively.

### 3.7. Co-Occurrence Analysis

To elucidate the potential adaptation mechanisms of wheat soil microbial communities to low-P and drought conditions, we examined the co-occurrence networks between bacteria and fungi under varying P fertilization and water availability conditions. Our analysis focused on the top 80 most abundant bacterial and fungal genera at the genus level, utilizing Spearman's correlation coefficients to depict the interrelationships among these genera.

In the bacterial networks, under drought conditions, P-deficient soil exhibited an increase in nodes and modularity while experiencing a decrease in the clustering coefficient, betweenness centralization, and graph density (Table S1). However, the average degree and degree centralization remained relatively stable, indicating an overall state of relative stability (Figure 5a).

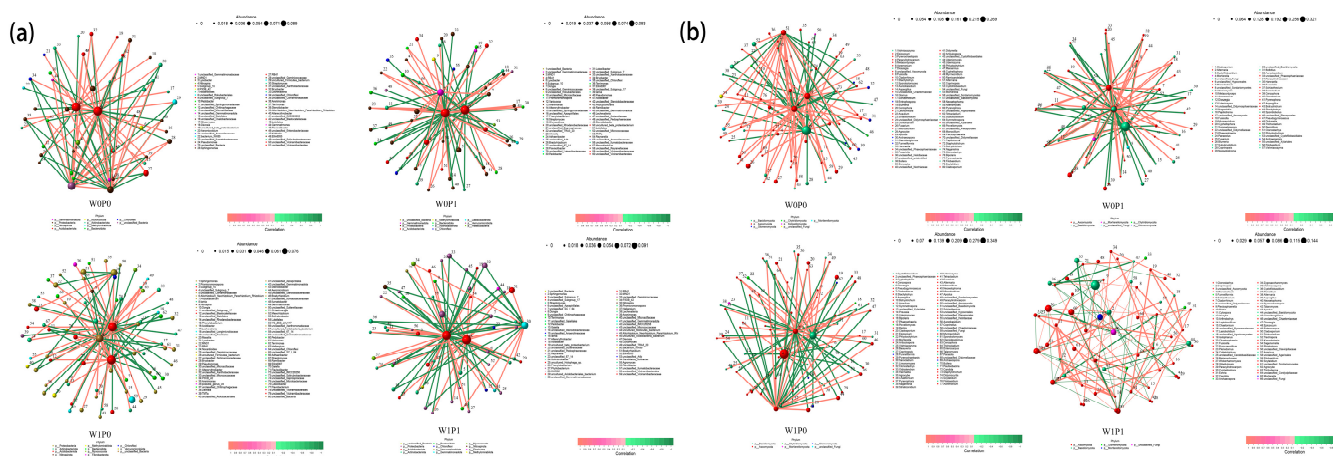


**Figure 5.** Network analysis showing the connectedness among bacterial genera based on 16S gene sequences (a) and fungal genera based on ITS gene sequences (b) in topsoil.

In the fungal network, under normal water conditions, P-deficient soil displayed an increase in nodes, average degree, clustering coefficient, and graph density (Table S2). Conversely, under drought conditions, the number of nodes and degree of centralization increased, whereas the clustering coefficient decreased. Additionally, under normal water conditions, drought enhanced the betweenness centralization and modularity of the fungal interaction network while leading to a decrease in nodes, average degree, clustering coefficient, and graph density (Figure 5b).

Co-occurrence network analysis was employed to compare the symbiotic relationships and community complexities of bacteria and fungi under different treatments (Figure 6). The topological network properties of microorganisms under different treatments are summarized in Table S3. When controlling the number of nodes at 100, it was observed that P deficiency under drought conditions increased the number of edges in the microbial network, whereas the opposite trend was observed under normal water conditions. Additionally, under drought conditions, P deficiency resulted in a higher proportion of positive correlations among the total edges, whereas the opposite pattern was observed under normal water conditions. These findings indicate that P deficiency, coupled with drought conditions, strengthens the symbiotic relationships between bacteria and fungi, thereby enhancing their ecological interdependencies and mutualistic associations.

### 3.8. Relationships Between the Soil Microbial Community and Wheat Yield

Environmental conditions are pivotal drivers of yield variability. To elucidate the direct and indirect relationships between environmental drivers and yield, we employed structural equation modeling to analyze the hypothesized interactions between these factors. In the model incorporating P as the driving factor (Figure 7A,C), pH (standardized

path coefficient,  $b = -0.090$ ) and SOC (standardized path coefficient,  $b = -0.679$ ) exhibited predominantly indirect negative effects on the yield. Conversely, P (standardized path coefficient,  $b = 0.708$ ), Ca-P (standardized path coefficient,  $b = 0.012$ ), and phosphatase activity (standardized path coefficient,  $b = 0.110$ ) demonstrated primarily indirect positive influences. Similarly, in the model with SWC (soil water content) as the driving factor (Figure 7B,D), Ca-P (standardized path coefficient,  $b = -0.031$ ) and SOC (standardized path coefficient,  $b = -1.006$ ) were associated with indirect negative effects on the yield. In contrast, SWC (standardized path coefficient,  $b = 0.264$ ) and Ca-P (standardized path coefficient,  $b = 0.405$ ) primarily contributed to indirect positive effects. In the model with P as the driving factor, the coefficient of determination ( $r^2$ ) of the bacterial community model was 0.231, and that of the fungal community model was 0.172. In the model with water as the driving factor, the coefficient of determination ( $r^2$ ) of the bacterial community model was 0.237, and that of the fungal community model was 0.173. The coefficient of determination of bacteria was higher than that of fungi. This suggests that the bacterial effects are more robust and exhibit stronger correlations in terms of model fit and statistical significance than those of the fungal communities.

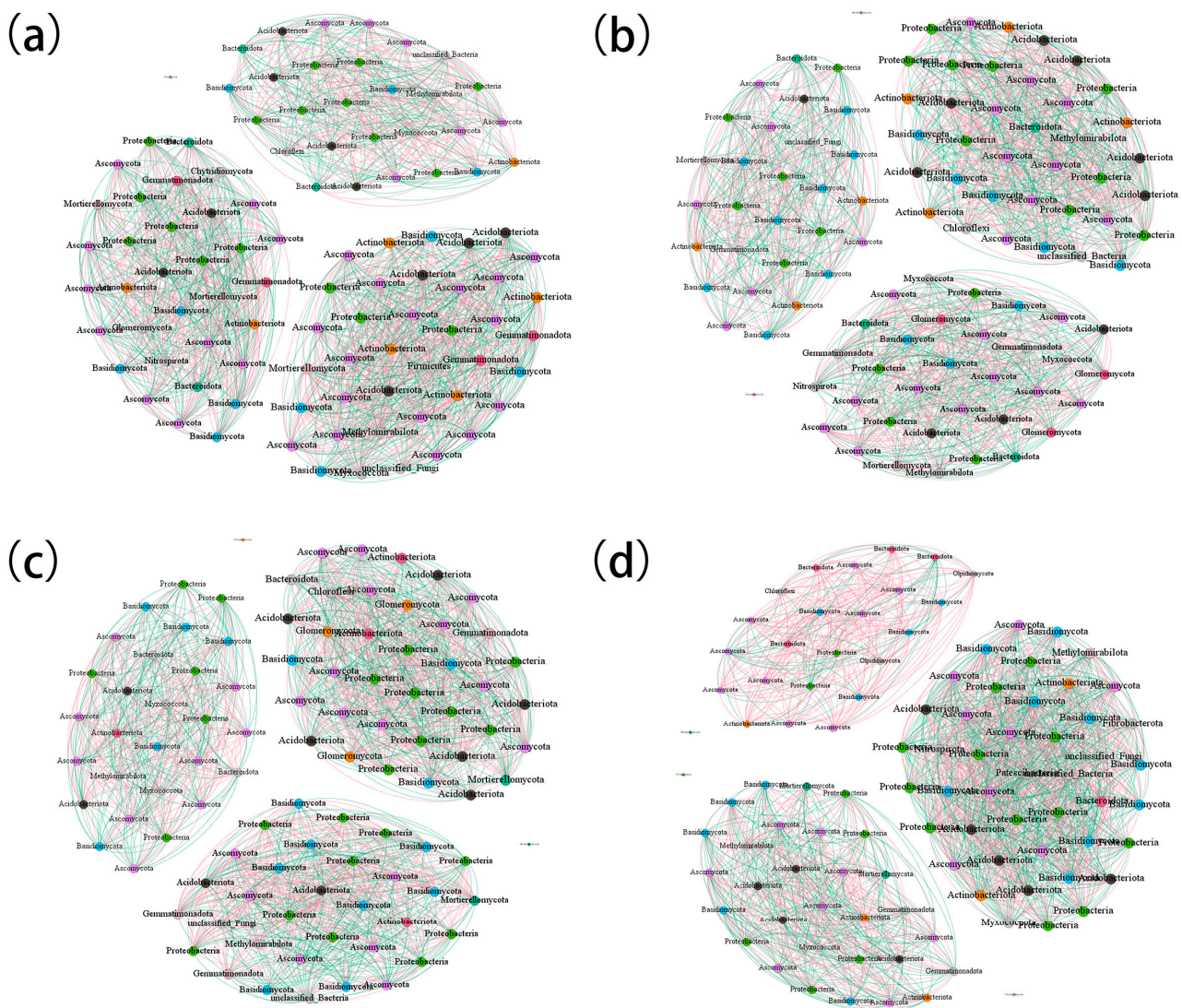


**Figure 6.** Co-occurrence network analysis of soil microbial communities in different treatments ((a), W0P0; (b), W0P1; (c), W1P0; (d), W1P1).



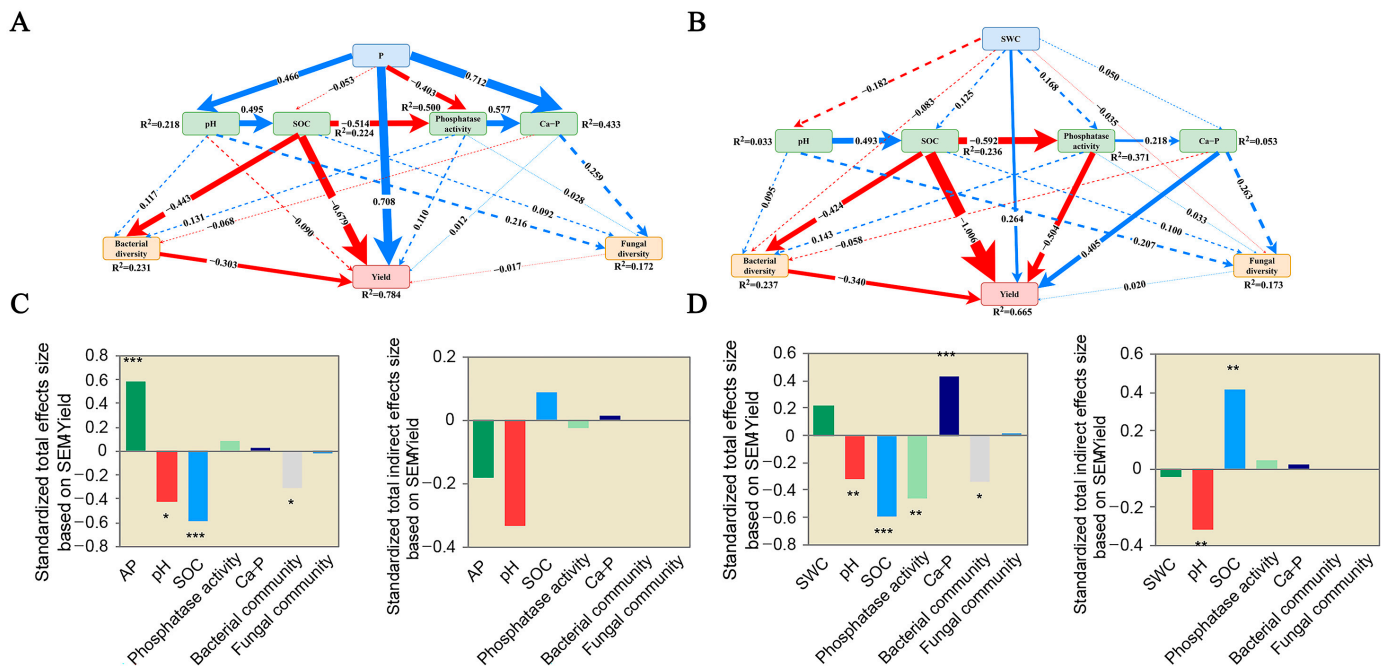


**Figure 7.** (A,B) Structural equation models (SEMs) showing the relationships among treatments, soil variables, and bacterial and fungal richness. Blue and red arrows indicate positive and negative relationships, respectively. Solid or dashed lines indicate significant ( $p < 0.05$ ) or non-significant relationships. Numbers near the pathway arrow indicate the standard path coefficients.  $R^2$  represents the proportion of variance explained for every dependent variable.  $\chi^2 = 47.69$ ,  $df. = 34$ ,  $p = 0.06$  (large  $p$  value indicates that the predicted model and observed data are equal, that is, good model fitting). Ca-P, the first principal component of Ca<sub>2</sub>-P, Ca<sub>8</sub>-P, Ca<sub>10</sub>-P; Bacterial and Fungal community, the first principal component of microbial abundance; Yield, the first principal component of grain yield, spike number, kernel number and 1000-kernel weight. (C,D) Standardized total effects and total indirect effects derived from SEMs.  $p$  values less than 0.001, 0.01, and 0.05 are indicated by the symbols of asterisks and dot as follows: “\*\*\*”, “\*\*” and “\*”.

#### 4. Discussion

By leveraging NovaSeq sequencing technology, we meticulously evaluated the variations and intricate interactions within the bacterial and fungal communities in wheat soil subjected to diverse P fertilizer treatments. Prolonged exposure to P deficiency, compounded by drought conditions, elicited discernible alterations in wheat growth and development and soil physicochemical attributes and significant shifts in the diversity, abundance metrics, community structure, and functionality of fungi and bacteria [27,28]. Such microbial shifts play a pivotal role in modulating nutrient utilization, tailoring soil properties, ameliorating plant growth, and maintaining ecological stability [29–31]. Notably, their instrumental roles in P cycling, particularly in augmenting P efficacy, cannot be overlooked [32,33]. Both bacteria and fungi contribute positively to wheat soil, particularly during P scarcity, facilitating the dissolution of certain sparingly soluble organic phosphates and proactively aiding plants in confronting P deficiency.

In our detailed investigation, which is consistent with previous studies [34], a conspicuous decline in soil pH was associated with P deficiency. This could be attributed to intensified nitrification reactions promoted by limited P or acidifying exudates (such as phosphatases) secreted by wheat in response to low-P conditions, aimed at enhancing phosphate dissolution and uptake [20,35,36]. Although the experiment determined that prolonged low-P conditions did not have a statistically significant effect on the overall P content in the soil, they profoundly influenced the content of certain recalcitrant and less bioavailable inorganic phosphates. Previous research has corroborated that, under exhaustive P conditions, the sparing utilization of divalent and octavalent calcium phos-

phates and the minimal chemical propensity of decavalent calcium phosphates render them highly unassailable [37,38]. The markedly lower levels of decavalent calcium phosphates under the WOP0 treatment compared with the other treatments indicated pronounced P depletion in the soil. However, the occluded P remained unchanged. The literature suggests that interconversions between occluded soil phosphates and other P forms are rather limited, reinforcing the stability and potential utility of these latent soil P reserves [39–41]. Delving deeper into the efficient conversion routes of soil-accumulated refractory phosphates to enhance P use efficiency and tap into the latent phosphorus pool holds significant promise. However, only a few studies have explored the intricate linkages between P and soil microbes.

Historical data suggest that both water and P exert a significant influence on the diversity and community composition of bacteria and fungi [27,42,43]. Certain nutrient-sensitive microbes may be curtailed, whereas less nutrient-dependent microbes may proliferate. However, the reciprocity of these microbial changes and their effects on the soil ecology warrant further exploration. Our findings revealed an upward trend in bacterial phyla such as *Acidobacteriota*, *unclassified\_Bacteria*, *Myxococcota*, *Methylomirabilota*, and *Chloroflex*, particularly *Acidobacteriota*, identified as oligotrophic groups capable of sustaining metabolic activities under nutrient-deprived conditions; however, certain bacterial genera, notably *unclassified\_Bacteria* and *unclassified\_Gemmatimonadaceae*, remain undefined but yet are perceived to be crucial in nutrient cycling and organic matter decomposition [44]. Bacteria, representing the most diverse and abundant taxa within soil microbes, promote plant growth, stabilize soil structure, and play an integral role in nutrient cycling [31,45]. The elucidating of their functional significance is indispensable for ecosystem stability. Fungal phyla like *Ascomycota*, *unclassified\_Fungi*, and *Glomeromycota* along with genera like *Scytalidium* are recognized for their critical role in sustaining nutrient stability under low-P conditions. The fungal content in the soil is lower than that of bacteria. However, in some specific soils, such as those of forests and those rich in organic matter, the relative abundance of fungi may be higher [46,47]. In other words, the effect value under low-nutrient conditions is less than that of bacteria.

Alterations in soil physicochemical characteristics significantly influence the composition of bacterial and fungal communities [48]. As illustrated in Figure 3, the majority of soil physicochemical attributes displayed linear relationships. The intricate phenomenon through which nutrient factors shape microbial community structures emerged as the central theme in our investigation. This study revealed a noticeable decrease in bacterial and fungal diversity under P-deficient conditions, with bacteria exhibiting a more pronounced response than fungi. Furthermore, symbiotic networks within microbial communities are indispensable in bolstering micro-ecological resilience and environmental equilibrium [49,50]. By constructing and scrutinizing the connectivity networks among species, we unveiled critical interspecific interactions and pivotal taxa. Empirical evidence indicates that environmental fluctuations, agronomic interventions, and the integration of exogenous organic matter can recalibrate the intricacy of soil microbial networks [51]. The introduction of organic matter augments the abundance and diversity of specific bacterial taxa within the soil, thereby fostering their interspecific interactions. Our findings highlight that both P and moisture regimes are determinants of microbial network intricacy and stability (Figure 6). Key taxa within microbial communities play a unique and pivotal role and their fluctuations can profoundly reconfigure the overall microbial network architecture and its associated functionalities [52–54]. Predicting the complexity of microbial interaction networks uncovers the labyrinth of interspecies dynamics, where a comprehensive understanding of such interactions is paramount for sustaining the stability and functionality of soil ecosystems [55].

Significant alterations in bacterial and fungal functions were identified in the functionality predictions performed in this study. Soil nutrient provision, especially C, N, and P, along with associated physicochemical indicators, can modulate the abundance of the P cycling functional gene, thereby influencing soil P utilization. Key functionalities, such as



cellular processes and metabolism, were highlighted for their significant roles under low-P and moisture-deficient conditions, with tertiary functions predominantly encompassing transcription, carbohydrate metabolism, and amino acid metabolism, corroborating the findings from previous studies [56,57]. The differences in secondary fungal functionalities were less pronounced than those in their bacterial counterparts, reiterating the hypothesis that bacteria potentially play a more vital role in ensuring environmental stability under P-deprived conditions.

## 5. Conclusions

This study elucidated the effects of chronic water and P deficiency on wheat photosynthesis and yield, soil physicochemical characteristics, and bacterial and fungal community composition. Long-term P deficiency significantly reduced wheat photosynthesis and yield, changed soil structure, and mobilized difficult-to-utilize inorganic phosphorus, such as Ca<sub>10</sub>P. Remarkably, bacteria and fungi emerged as pivotal actors in effectively navigating soil P conditions, reaffirming the prevailing notion that bacteria have a superior influence on soil stress compared with fungi. Moreover, P exerted a pronounced influence on symbiotic associations and crucial taxa that dictate network stability within bacterial and fungal communities. Furthermore, research endeavors were made to prognosticate the functional repercussions of both fungal and bacterial cohorts. By delving into the intricacies of microbial interplay networks, profound insights into the intricate modes of microbial interactions can be gained, thereby enabling enhanced soil ecosystem management, elevated agricultural productivity, and the advancement of sustainable soil stewardship.

**Supplementary Materials:** The following supporting information can be downloaded at: <https://www.mdpi.com/article/10.3390/agriculture14112022/s1>, Figure S1: Non-metric multi-dimensional scaling (NMDS) plots of bacterial (a) and fungus (b) communities based on Bray-Curtis dissimilarities; Figure S2: Rarefaction curves of (a) 16S rRNA genes and (b) ITS genes; Figure S3: LEfSe analysis results showed that there were significant differences in soil bacterial groups (a) and fungal communities (b) under the four treatments; Cladogram plotted from LEfSe analysis showing significant differences ( $p < 0.05$ ) in relative abundance of ITS gene-based bacterial taxa (c) and fungal taxa (d) across the five treatments; Table S1: Topological properties of collinear network of soil bacterial communities; Table S2: Topological properties of collinear network of soil fungal communities; Table S3: Topological properties of collinear network of soil bacterial and fungal communities.

**Author Contributions:** J.H.: Methodology, Data collection, Writing—Original draft preparation. T.L. and Z.W.: Conceptualization and Supervision. Y.L. and Y.R.: Writing—Review and Editing. Z.L., H.P., H.G. and M.Z.: Revised the manuscript. All authors have read and agreed to the published version of the manuscript.

**Funding:** This study was financially supported by the National Key Research and Development Program of China (2022YFD2300803-3), the National Natural Science Foundation of China (32201907).

**Institutional Review Board Statement:** Not applicable.

**Data Availability Statement:** Data will be made available on request.

**Conflicts of Interest:** The authors declare that they have no known competing financial interests or personal relationships that could have appeared to influence the work reported in this paper.

## References

1. Langhans, C.; Beusen, A.H.W.; Mogollón, J.M.; Bouwman, A.F. Phosphorus for Sustainable Development Goal target of doubling smallholder productivity. *Nat. Sustain.* **2022**, *5*, 57–63. [CrossRef]
2. Kang, J.; Chu, Y.; Ma, G.; Zhang, Y.; Zhang, X.; Wang, M.; Lu, H.; Wang, L.; Kang, G.; Ma, D.; et al. Physiological mechanisms underlying reduced photosynthesis in wheat leaves grown in the field under conditions of nitrogen and water deficiency. *Crop J.* **2023**, *11*, 638–650. [CrossRef]
3. Li, L.; Li, S.-M.; Sun, J.-H.; Zhou, L.-L.; Bao, X.-G.; Zhang, H.-G.; Zhang, F.-S. Diversity enhances agricultural productivity via rhizosphere phosphorus facilitation on phosphorus-deficient soils. *Proc. Natl. Acad. Sci. USA* **2007**, *104*, 11192–11196. [CrossRef]

4. Wilpiseski, R.L.; Aufrecht, J.A.; Retterer, S.T.; Sullivan, M.B.; Graham, D.E.; Pierce, E.M.; Zablocki, O.D.; Palumbo, A.V.; Elias, D.A. Soil Aggregate Microbial Communities: Towards Understanding Microbiome Interactions at Biologically Relevant Scales. *Appl. Environ. Microbiol.* **2019**, *85*, e00324-19. [CrossRef]
5. Shen, J.; Yuan, L.; Zhang, J.; Li, H.; Bai, Z.; Chen, X.; Zhang, W.; Zhang, F. Phosphorus dynamics: From soil to plant. *Plant Physiol.* **2011**, *156*, 997–1005. [CrossRef]
6. Swanson, S.; Gilroy, S. *Calcium: From Root Macronutrient to Mechanical Signal*; CRC Press: Boca Raton, FL, USA, 2013. [CrossRef]
7. Liu, J.; Ma, Q.; Hui, X.; Ran, J.; Ma, Q.; Wang, X.; Wang, Z. Long-term high-P fertilizer input decreased the total bacterial diversity but not phoD-harboring bacteria in wheat rhizosphere soil with available-P deficiency. *Soil Biol. Biochem.* **2020**, *149*, 107918. [CrossRef]
8. Cheng, H.; Yuan, M.; Tang, L.; Shen, Y.; Yu, Q.; Li, S. Integrated microbiology and metabolomics analysis reveal responses of soil microorganisms and metabolic functions to phosphorus fertilizer on semiarid farm. *Sci. Total Environ.* **2022**, *817*, 152878. [CrossRef]
9. Qiu, H.; Mei, X.; Liu, C.; Wang, J.; Wang, G.; Wang, X.; Liu, Z.; Cai, Y. Fine mapping of quantitative trait loci for acid phosphatase activity in maize leaf under low phosphorus stress. *Mol. Breed.* **2013**, *32*, 629–639. [CrossRef]
10. Dai, Z.; Liu, G.; Chen, H.; Chen, C.; Wang, J.; Ai, S.; Wei, D.; Li, D.; Ma, B.; Tang, C.; et al. Long-term nutrient inputs shift soil microbial functional profiles of phosphorus cycling in diverse agroecosystems. *ISME J.* **2020**, *14*, 757–770. [CrossRef]
11. Wang, J.; Liu, W.-Z.; Mu, H.-F.; Dang, T.-H. Inorganic Phosphorus Fractions and Phosphorus Availability in a Calcareous Soil Receiving 21-Year Superphosphate Application. *Pedosphere* **2010**, *20*, 304–310. [CrossRef]
12. Piegholdt, C.; Geisseler, D.; Koch, H.J.; Ludwig, B. Long-term tillage effects on the distribution of phosphorus fractions of loess soils in Germany. *J. Plant Nutr. Soil Sci.* **2013**, *176*, 217–226. [CrossRef]
13. Liu, Z.-P.; Shao, M.-A.; Wang, Y.-Q. Spatial patterns of soil total nitrogen and soil total phosphorus across the entire Loess Plateau region of China. *Geoderma* **2013**, *197–198*, 67–78. [CrossRef]
14. Sinclair, T.R.; Ruffly, T.W. Nitrogen and water resources commonly limit crop yield increases, not necessarily plant genetics. *Glob. Food Secur.* **2012**, *1*, 94–98. [CrossRef]
15. Chen, W.; Zhou, H.; Wu, Y.; Wang, J.; Zhao, Z.; Li, Y.; Qiao, L.; Chen, K.; Liu, G.; Xue, S. Direct and indirect influences of long-term fertilization on microbial carbon and nitrogen cycles in an alpine grassland. *Soil Biol. Biochem.* **2020**, *149*, 107922. [CrossRef]
16. Spohn, M.; Treichel, N.S.; Cormann, M.; Schloter, M.; Fischer, D. Distribution of phosphatase activity and various bacterial phyla in the rhizosphere of *Hordeum vulgare* L. depending on P availability. *Soil Biol. Biochem.* **2015**, *89*, 44–51. [CrossRef]
17. Dan, A.; Zhang, N.; Qiu, R.; Li, C.; Wang, S.; Ni, Z. Accelerated biodegradation of p-tert-butylphenol in the Phragmites australis rhizosphere by phenolic root exudates. *Environ. Exp. Bot.* **2020**, *169*, 103891. [CrossRef]
18. Su, J.-Q.; Ding, L.-J.; Xue, K.; Yao, H.-Y.; Quensen, J.; Bai, S.-J.; Wei, W.-X.; Wu, J.-S.; Zhou, J.; Tiedje, J.M.; et al. Long-term balanced fertilization increases the soil microbial functional diversity in a phosphorus-limited paddy soil. *Mol. Ecol.* **2015**, *24*, 136–150. [CrossRef]
19. Li, H.; Bi, Q.; Yang, K.; bo Lasson, S.; Zheng, B.; Cui, L.; Zhu, Y.; Ding, K. High starter phosphorus fertilization facilitates soil phosphorus turnover by promoting microbial functional interaction in an arable soil. *J. Environ. Sci.* **2020**, *94*, 179–185. [CrossRef]
20. Santoro, V.; Schiavon, M.; Visentin, I.; Constan-Aguilar, C.; Cardinale, F.; Celi, L. Strigolactones affect phosphorus acquisition strategies in tomato plants. *Plant Cell Environ.* **2021**, *44*, 3628–3642. [CrossRef]
21. Dixon, M.; Simonne, E.; Obreza, T.; Liu, G. Crop Response to Low Phosphorus Bioavailability with a Focus on Tomato. *Agronomy* **2020**, *10*, 617. [CrossRef]
22. Lu, R. Methods for Agrochemical Analysis of Soils. 2000. Available online: <https://www.hanspub.org/reference/referencepapers?ReferenceID=6086> (accessed on 14 October 2024).
23. Hedley, M.J.; Stewart, J.W.B.; Chauhan, B.S. Changes in Inorganic and Organic Soil Phosphorus Fractions Induced by Cultivation Practices and by Laboratory Incubations. *Soil Sci. Soc. Am. J.* **1982**, *46*, 970–976. [CrossRef]
24. Mori, H.; Maruyama, F.; Kato, H.; Toyoda, A.; Dozono, A.; Ohtsubo, Y.; Nagata, Y.; Fujiyama, A.; Tsuda, M.; Kurokawa, K. Design and Experimental Application of a Novel Non-Degenerate Universal Primer Set that Amplifies Prokaryotic 16S rRNA Genes with a Low Possibility to Amplify Eukaryotic rRNA Genes. *DNA Res.* **2014**, *21*, 217–227. [CrossRef] [PubMed]
25. Zhang, S.; Song, X.; Li, N.; Zhang, K.; Liu, G.; Li, X.; Wang, Z.; He, X.; Wang, G.; Shao, H. Influence of high-carbon basal fertiliser on the structure and composition of a soil microbial community under tobacco cultivation. *Res. Microbiol.* **2018**, *169*, 115–126. [CrossRef]
26. Wemheuer, F.; Taylor, J.A.; Daniel, R.; Johnston, E.; Wemheuer, B. Tax4Fun2: A R-based tool for the rapid prediction of habitat-specific functional profiles and functional redundancy based on 16S rRNA gene marker gene sequences. *bioRxiv* **2018**. [CrossRef]
27. Chen, J.; Wu, Q.; Li, S.; Ge, J.; Liang, C.; Qin, H.; Xu, Q.; Fuhrmann, J.J. Diversity and function of soil bacterial communities in response to long-term intensive management in a subtropical bamboo forest. *Geoderma* **2019**, *354*, 113894. [CrossRef]
28. Gu, Y.; Ros, G.H.; Zhu, Q.; Zheng, D.; Shen, J.; Cai, Z.; Xu, M.; de Vries, W. Responses of total, reactive and dissolved phosphorus pools and crop yields to long-term fertilization. *Agric. Ecosyst. Environ.* **2023**, *357*, 108658. [CrossRef]
29. Sharma, S.B.; Sayyed, R.Z.; Trivedi, M.H.; Gobi, T.A. Phosphate solubilizing microbes: Sustainable approach for managing phosphorus deficiency in agricultural soils. *Springerplus* **2013**, *2*, 587. [CrossRef]

30. Zhu, W.-B.; Zhao, X.; Wang, S.-Q.; Wang, Y. Inter-annual variation in P speciation and availability in the drought-rewetting cycle in paddy soils. *Agric. Ecosyst. Environ.* **2019**, *286*, 106652. [CrossRef]
31. Chen, J.; Gong, J.; Xu, M. Implications of continuous and rotational cropping practices on soil bacterial communities in pineapple cultivation. *Eur. J. Soil Biol.* **2020**, *97*, 103172. [CrossRef]
32. Yuan, J.; Wang, L.; Chen, H.; Chen, G.; Wang, S.; Zhao, X.; Wang, Y. Responses of soil phosphorus pools accompanied with carbon composition and microorganism changes to phosphorus-input reduction in paddy soils. *Pedosphere* **2021**, *31*, 83–93. [CrossRef]
33. Yuan, J.; Wang, Y.; Zhao, X.; Chen, H.; Chen, G.; Wang, S. Seven years of biochar amendment has a negligible effect on soil available P and a progressive effect on organic C in paddy soils. *Biochar* **2022**, *4*, 1. [CrossRef]
34. Zhang, X.; Wei, H.; Chen, Q.; Han, X. The counteractive effects of nitrogen addition and watering on soil bacterial communities in a steppe ecosystem. *Soil Biol. Biochem.* **2014**, *72*, 26–34. [CrossRef]
35. Czarnecki, O.; Yang, J.; Weston, D.J.; Tuskan, G.A.; Chen, J.-G. A Dual Role of Strigolactones in Phosphate Acquisition and Utilization in Plants. *Int. J. Mol. Sci.* **2013**, *14*, 7681–7701. [CrossRef]
36. Joshi, S.R.; Morris, J.W.; Tfaily, M.M.; Young, R.P.; Mcnear, D.H. Low soil phosphorus availability triggers maize growth stage specific rhizosphere processes leading to mineralization of organic P. *Plant Soil* **2021**, *459*, 423–440. [CrossRef]
37. Richardson, A.E.; Barea, J.-M.; McNeill, A.M.; Prigent-Combaret, C. Acquisition of phosphorus and nitrogen in the rhizosphere and plant growth promotion by microorganisms. *Plant Soil* **2009**, *321*, 305–339. [CrossRef]
38. Sánchez Rodríguez, A.R. *Influencia de la Fertilización Fosfatada en la Clorosis Férrica*; Universidad de Córdoba, Servicio de Publicaciones: Córdoba, Spain, 2013. Available online: <http://hdl.handle.net/10396/11410> (accessed on 1 November 2024).
39. Sharpley, A.N.; McDowell, R.W.; Kleinman, P.J.A. Amounts, Forms, and Solubility of Phosphorus in Soils Receiving Manure. *Soil Sci. Soc. Am. J.* **2004**, *68*, 2048–2057. [CrossRef]
40. Richardson, A.E.; Hocking, P.J.; Simpson, R.J.; George, T.S. Plant mechanisms to optimise access to soil phosphorus. *Crop Pasture Sci.* **2009**, *60*, 124–143. [CrossRef]
41. Faucon, M.-P.; Houben, D.; Lambers, H. Plant Functional Traits: Soil and Ecosystem Services. *Trends Plant Sci.* **2017**, *22*, 385–394. [CrossRef]
42. Kielak, A.M.; Barreto, C.C.; Kowalchuk, G.A.; van Veen, J.A.; Kuramae, E.E. The Ecology of Acidobacteria: Moving beyond Genes and Genomes. *Front. Microbiol.* **2016**, *7*, 744. [CrossRef]
43. Lladó, S.; López-Mondéjar, R.; Baldrian, P. Forest Soil Bacteria: Diversity, Involvement in Ecosystem Processes, and Response to Global Change. *Microbiol. Mol. Biol. Rev. MMBR* **2017**, *81*, e00063-16. [CrossRef]
44. Eichorst, S.A.; Trojan, D.; Roux, S.; Herbold, C.; Rattei, T.; Wobken, D. Genomic insights into the Acidobacteria reveal strategies for their success in terrestrial environments. *Environ. Microbiol.* **2018**, *20*, 1041–1063. [CrossRef] [PubMed]
45. Ma, G.; Kang, J.; Wang, J.; Chen, Y.; Lu, H.; Wang, L.; Wang, C.; Xie, Y.; Ma, D.; Kang, G. Bacterial Community Structure and Predicted Function in Wheat Soil From the North China Plain Are Closely Linked with Soil and Plant Characteristics After Seven Years of Irrigation and Nitrogen Application. *Front. Microbiol.* **2020**, *11*, 506. [CrossRef] [PubMed]
46. Tedersoo, L.; Bahram, M.; Põlme, S.; Kõljalg, U.; Yorou, N.S.; Wijesundera, R.; Ruiz, L.V.; Vasco-Palacios, A.M.; Thu, P.Q.; Suija, A.; et al. Global diversity and geography of soil fungi. *Science* **2014**, *346*, 1256688. [CrossRef] [PubMed]
47. Baldrian, P. Forest microbiome: Diversity, complexity and dynamics. *FEMS Microbiol. Rev.* **2017**, *41*, 109–130. [CrossRef]
48. Liu, M.; Liu, J.; Jiang, C.; Wu, M.; Song, R.; Gui, R.; Jia, J.; Li, Z. Improved nutrient status affects soil microbial biomass, respiration, and functional diversity in a Lei bamboo plantation under intensive management. *J. Soils Sediments* **2017**, *17*, 917–926. [CrossRef]
49. Zheng, W.; Zhao, Z.; Gong, Q.; Zhai, B.; Li, Z. Responses of fungal–bacterial community and network to organic inputs vary among different spatial habitats in soil. *Soil Biol. Biochem.* **2018**, *125*, 54–63. [CrossRef]
50. Jiao, S.; Peng, Z.; Qi, J.; Gao, J.; Wei, G. Linking Bacterial-Fungal Relationships to Microbial Diversity and Soil Nutrient Cycling. *mSystems* **2021**, *6*, e01052-20. [CrossRef]
51. Li, B.-B.; Roley, S.S.; Duncan, D.S.; Guo, J.; Quensen, J.F.; Yu, H.-Q.; Tiedje, J.M. Long-term excess nitrogen fertilizer increases sensitivity of soil microbial community to seasonal change revealed by ecological network and metagenome analyses. *Soil Biol. Biochem.* **2021**, *160*, 108349. [CrossRef]
52. Lu, L.; Yin, S.; Liu, X.; Zhang, W.; Gu, T.; Shen, Q.; Qiu, H. Fungal networks in yield-invigorating and -debilitating soils induced by prolonged potato monoculture. *Soil Biol. Biochem.* **2013**, *65*, 186–194. [CrossRef]
53. Freilich, M.A.; Wieters, E.; Broitman, B.R.; Marquet, P.A.; Navarrete, S.A. Species co-occurrence networks: Can they reveal trophic and non-trophic interactions in ecological communities? *Ecology* **2018**, *99*, 690–699. [CrossRef]
54. Luo, J.; Banerjee, S.; Ma, Q.; Liao, G.; Hu, B.; Zhao, H.; Li, T. Organic fertilization drives shifts in microbiome complexity and keystone taxa increase the resistance of microbial mediated functions to biodiversity loss. *Biol. Fertil. Soils* **2023**, *59*, 441–458. [CrossRef]
55. Suleiman, A.K.A.; Gonzatto, R.; Aita, C.; Lupatini, M.; Jacques, R.J.S.; Kuramae, E.E.; Antonioli, Z.I.; Roesch, L.F.W. Temporal variability of soil microbial communities after application of dicyandiamide-treated swine slurry and mineral fertilizers. *Soil Biol. Biochem.* **2016**, *97*, 71–82. [CrossRef]

56. Fierer, N.; Leff, J.W.; Adams, B.J.; Nielsen, U.N.; Bates, S.T.; Lauber, C.L.; Owens, S.; Gilbert, J.A.; Wall, D.H.; Caporaso, J.G. Cross-biome metagenomic analyses of soil microbial communities and their functional attributes. *Proc. Natl. Acad. Sci. USA* **2012**, *109*, 21390–21395. [[CrossRef](#)] [[PubMed](#)]
57. Fitzpatrick, C.R.; Mustafa, Z.; Viliunas, J. Soil microbes alter plant fitness under competition and drought. *J. Evol. Biol.* **2019**, *32*, 438–450. [[CrossRef](#)]

**Disclaimer/Publisher’s Note:** The statements, opinions and data contained in all publications are solely those of the individual author(s) and contributor(s) and not of MDPI and/or the editor(s). MDPI and/or the editor(s) disclaim responsibility for any injury to people or property resulting from any ideas, methods, instructions or products referred to in the content.